Plant community functional composition and diversity drive fine-scale variability in carbon cycling in the tundra

Konsta Happonen*, Anna-Maria Virkkala*, Julia Kemppinen, Pekka Niittynen & Miska Luoto

*These authors contributed equally to this work.

Department of Geosciences and Geography, University of Helsinki

P.O.Box 64, Gustaf Hällströmin katu 2, 00014 University of Helsinki, Finland

Authors for correspondence:

Konsta Happonen, konsta.happonen@gmail.com, +358452591889, or

Anna-Maria Virkkala, anna-maria.virkkala@helsinki.fi, +358445441040

Total word count: 6201 words, consisting of

Introduction, 997 words,

Materials and Methods, 3050 words,

Results, 520 words,

Discussion, 1480 words, and

Acknowledgements, 154 words.

Figures published in colour: 6

Tables: 1

Supporting information: one file with Figures S1–S4, and Methods S1–S3.

Summary

- We investigated how plant functional traits influence fine-scale patterns of tundra carbon cycling, and how carbon cycling responds to climate warming.
- We built a hierarchical model that included abiotic conditions (summer air and winter soil temperatures, and soil resources), plant community functional composition and diversity (plant size and leaf economics), and carbon cycling (above-ground and soil organic carbon stocks, and photosynthetic and respiratory fluxes). We also simulated warming effects on the peak-season CO_2 budget.
- Plant size was the strongest predictor for most carbon cycling variables. Communities of larger plants were associated with larger CO_2 fluxes and above-ground carbon stocks. Communities with fast leaf economics had higher rates of photosynthesis and soil respiration, but lower soil organic carbon stocks. Leaf economic diversity increased CO_2 fluxes, while size diversity increased the above-ground carbon stock. Simulations suggested that warmer summer air temperatures increase plant size and accelerate leaf economics, while warmer winter soil temperatures increase plant size. Both changes would enhance CO_2 uptake during the peak season.
- We show that traits act as mediators between abiotic conditions and carbon cycling. Our study firmly links the trait composition and diversity of plant communities to ecosystem functions in the tundra.

Key words

Alpine, Arctic, biodiversity, carbon dioxide exchange, LDMC, plant height, soil respiration vegetation

Introduction

The Arctic is warming two to four times faster than the planet on average (Holland & Landrum, 2015), leading to changes in plant growth (Myers-Smith *et al.*, 2015), height (Bjorkman *et al.*, 2018a), and species distributions (Steinbauer *et al.*, 2018). It is unclear how such changes in vegetation will influence the carbon balance of these ecosystems. On one hand, the expansion of larger plants might increase net carbon uptake (Cahoon *et al.*, 2012; Sørensen *et al.*, 2017). On the other hand, vegetation-driven changes in soil conditions might

accelerate decomposition and, in turn, increase carbon losses to the atmosphere (Parker *et al.*, 2015). Tundra soils contain more than half of the global soil organic carbon stock (Hugelius *et al.*, 2014), thus changes in tundra carbon cycling have the potential to influence atmospheric CO_2 concentrations at the global scale.

By virtue of their sheer mass, plants are the most important regulators of terrestrial carbon cycling (Bar-On *et al*., 2018). In recent years, plants and the communities they form have begun to be characterized by their functional traits. Functional traits are a means to link community composition to environmental conditions and ecosystem functioning (Lavorel & Garnier, 2002). Because traits are less constrained by the species pool (Villéger *et al.*, 2013) or by stochastic variation (Messier *et al*., 2010) than species composition and diversity, traits can act as a common currency by which it is possible to compare sets of unique species (McGill *et al.*, 2006).

Above-ground traits of plant species and the functional composition of plant communities have been found to vary primarily along two axes (Díaz *et al.*, 2016; Bruelheide *et al.*, 2018). The first axis describes the trade-offs between resource acquisitive and resource conservative strategies, and has often been called the leaf economics spectrum (Wright *et al*., 2004). The other axis is related to plant size (Díaz *et al*., 2016). These trait axes explain differences between species' vital rates that define population processes (Adler *et al.*, 2014), and also ecosystem functioning from local to global scales (Díaz *et al*., 2004; Michaletz *et al*., 2014). In the tundra, however, only a handful of studies have focused on linking traits to carbon cycling (e.g. Sharp *et al*., 2013; Sørensen *et al*., 2019).

Most of the studies examining traits and ecosystem functioning are based on the dominance hypothesis (i.e. the mass ratio hypothesis, Grime, 1998), which states that ecosystem processes are determined by the trait values of dominant species in the community. However, according to the niche complementarity hypothesis (i.e. diversity hypothesis, Tilman *et al.*, 1997), the diversity of communities also influences ecosystem processes. Both experimental and observational studies strongly agree that ecosystem functioning generally increases along with the diversity of local species assemblages (Tilman *et al*., 2014; Duffy *et al*., 2017). There are many possible reasons for this relationship, most of which invoke increasing resource-use efficiency with increasing number of species. Using functional traits allows partitioning of the diversity effect on ecosystem functioning to contributions from

complementarity along different niche axes (Cadotte *et al.*, 2011). This increases our understanding of the causes of diversity-functioning relationships in different contexts.

Biodiversity-ecosystem functioning has most often been quantified with net primary productivity (NPP) as the response variable (Tilman *et al.*, 2014). However, NPP is the sum of CO_2 gain by photosynthesis and CO_2 loss through plant respiration. Both photosynthesis and respiration are intimately linked to other flows of matter, such as water and nutrient uptake, nutrient circulation, and root exudation. Hence, NPP as a measure of ecosystem functioning can be slightly misleading: small NPP can result from large carbon gains and losses, as long as photosynthesis and plant respiration are of roughly equal magnitude. Biodiversity-ecosystem functioning research would benefit from more frequent direct studying of the processes that make up NPP.

Carbon cycling comprises fluxes (flows) and stocks (quantities) both above- and below-ground, which are linked to trait variation (Garnier *et al.*, 2004). Nevertheless, most carbon cycling studies have not described the functional properties of vegetation with ecologically meaningful variables. Instead they have relied on coarser proxies, such as plant functional groups or vegetation classification (Virkkala *et al.*, 2018). Recent research has shown that these approaches might ignore large variation in vegetation properties that are relevant for ecosystem functioning (Cadotte *et al.*, 2011; Thomas *et al.*, 2019). Furthermore, the use of classification methods makes it impractical to compare the results of independent studies if their classifications differ. Using globally applicable quantitative plant functional traits is a solution to both problems.

In addition to the need to clarify the way we describe vegetation-carbon cycling relationships, there is also a need to account for the hierarchy of processes controlling ecosystem functioning. The impacts of climate change on ecosystem functioning are not always straightforward. For example, modern climate change is causing seemingly contradictory responses in the productivity of Arctic ecosystems, such as “greening” and shrub encroachment (Jia *et al.*, 2003; Myers-Smith *et al.*, 2011), and “browning” and vegetation dieback (Phoenix & Bjerke, 2016). A hierarchical framework could allow the factors controlling vegetation changes and carbon cycling in this complex system to be teased apart (Díaz *et al.*, 2007). To our knowledge, such an approach has not been considered much thus far. A deeper understanding of the proximate (vegetation) and ultimate (environment) drivers

of carbon cycling is therefore needed to identify climate change -related feedbacks in Arctic ecosystems.

In this study, we examine the relationships between abiotic environmental conditions, plant community functional composition and diversity, and carbon cycling in a tundra landscape using a unique study setting of 87–200 intensively measured plots and coupled Bayesian regression models. To understand carbon cycling comprehensively, we focus not only on CO_2 fluxes (gross primary productivity, ecosystem respiration, soil respiration), but also on carbon stocks (above-ground and soil organic carbon stocks; for abbreviations used in materials and methods, and results, see Table 1). Finally, we simulate how summer and winter warming could cause cascading effects on the carbon uptake capacity of the ecosystem, measured as the peak-season CO_2 budget.

Materials and Methods

Study site

The field observations for this study were collected in 2016–2018 in an oroarctic tundra environment in Kilpisjärvi, northwestern Finland (Fig. 1). The study area is located in an elevational gradient between two mountains, Saana (1029 m.a.s.l) and Korkea-Jehkats (960 m.a.s.l), and the valley in between (*ca.* 600 m.a.s.l). The study design consisted of 220 locations in a 1.5 x 2.0 km area (Fig. 1). The distance between two adjacent locations was a minimum of 23 m (average 101 m). Individual study locations were thus in separate vegetation patches.

The study area is above the mountain birch (*Betula pubescens* var. *pumila* (L.) Govaerts) forest line, and is dominated by dwarf-shrub heaths. *Empetrum nigrum* L., *Betula nana* L., *Vaccinium myrtillus* L., *Vaccinium vitis-idaea* L. and *Phyllodoce caeruleae* (L.) Bab. are highly abundant in the area. The abundance of herbs and graminoids is fairly low and is concentrated around meltwater streams. The main herbivores in the area are reindeer (*Rangifer tarandus tarandus* L.), and voles and lemmings (Cricetidae). Mean annual temperature in Saana (1002 m.a.s.l) is -3.1□ and annual rainfall at a nearby meteorological station (Kilpisjärvi kyläkeskus, 480 m.a.s.l) is 518 mm (1991–2018; Finnish Meteorological Institute, 2019a,b). The mean annual temperature in Kilpisjärvi has increased from *ca.* -3 to -1□ between 1980 and 2018 (Finnish Meteorological Institute, 2019b).

Abiotic variables: PAR, microclimate, soil moisture, soil pH

At the study area, we measured Photosynthetically Active Radiation (PAR) using a PAR Light Quantum Sensor 3668I (Spectrum Technologies, Inc., USA; PPFD range 0–2500 µmol m^2 s^{-1}, ±5%) with a WatchDog Data Logger 2000 (Spectrum Technologies, Inc., USA). The sensor recorded PAR as photosynthetic photon flux density (PPFD, µmol m^2 s^{-1}) every 10 minutes from July 9th to August 17th 2017. For more information see Supporting Information, Methods S1.

We chose to explain traits and carbon cycling with variables that previous research has shown to be important (Happonen *et al.*, 2019). These were soil resources (Shaver *et al.*, 1992), summer microclimate (Cahoon *et al.*, 2012), and winter temperatures that are influenced by snow conditions (Nobrega & Grogan, 2007).

Soil moisture was measured during the growing seasons of 2016–2018 in 220 locations, 3–6 times per growing season (Kemppinen *et al.*, 2018; Happonen *et al.*, 2019). Before the soil moisture measurements, there were no precipitation events in the preceding 24 hours. In each study location, moisture was measured from five 1 m^2 plots: one central plot and one plot 5 m away in each cardinal direction. In each plot, three measurements were taken, and the average was used in further analyses. Measurements were taken using a handheld time-domain reflectometry sensor of the accuracy ±3.0 VWC% with 0.1 VWC% resolution (FieldScout TDR 300; Spectrum Technologies Inc., Plainfield, IL, USA). Temperature loggers (Thermochron iButton DS1921G and DS1922L; temperature range between -40 and 85°C, resolution of 0.5°C, and accuracy of 0.5°C) were installed in 112 locations to monitor temperatures 10 cm above and below-ground, at 2–4 h intervals. These single time-point measurements were consequently aggregated to monthly averages.

To quantify average summer and winter temperatures and soil moisture conditions, we averaged July air temperatures, average February soil temperatures, and growing season soil moisture levels over several years for each location using random effects models with the R package lme4 (version 1.1-18-1, Bates *et al.*, 2015). We chose July and February because they are respectively the warmest and coldest months in the area. We used soil instead of air

temperature to characterize winter temperature conditions because during that time, most plants are protected by a thick layer of snow.

Random effect modelling allows the use of hierarchical structure in the data to pool information over those hierarchies, in this case years and locations. Thus, calculated averages are also more robust to outlier observations than normal arithmetic averaging. Air and soil temperatures were modelled using location and year as random effects (y ~ 1|location + year). Soil moisture was modelled using plot nested in location, and year as random effects (y ~ 1|location/plot + year). Soil moisture was $\log_e$-transformed before modelling. Finally, the environmental variables were predicted for the location (air and soil temperatures), or for the central plot of the moisture measurement scheme (soil moisture). Soil moisture was back-transformed before further analyses.

Samples of the organic soil layer were collected from 200 locations (for more details see section Carbon stock data). Soil samples were freeze-dried, and pH was analyzed from the samples in the laboratory of the University of Helsinki, following (ISO 10390, 2005) standard.

The average soil moisture and pH of the organic layer were highly correlated ($\rho > 0.8$). Hence, we reduced them to their first principal component, which we hereafter refer to as the soil resource axis. The final predictors used in the analysis were thus named summer temperature (average July air temperatures), winter temperature (average February soil temperatures) and soil resources (first principal component of soil moisture and soil pH).

Vegetation data: trait and community data

We quantified vascular plant community species composition in 143 of the plots where CO_2 flux measurements were conducted (see section CO_2 flux data) using the point-intercept method. These data have previously been used to study the relationship between the environment and functional composition (Happonen *et al.*, 2019). A circular frame (20 cm diameter) with 20 evenly spaced pinholes was placed over the soil collar (see section CO_2 flux data) after gas exchange measurements. The total number of times each species touched pins (3 mm in thickness) lowered into the vegetation through the frame was counted and used as a measurement of species abundance.

We measured plot-specific plant height and LDMC for all species (Happonen *et al*. 2019). We chose height and LDMC because they are good indicators of the two axes of functional differentiation of plant communities: size and the leaf economic spectrum (Bruelheide *et al.*, 2018). Trait measurements were done separately for all locations, and always on plant individuals within the soil collars in order to account for intraspecific trait variation.

Height was quantified as the height of the highest leaf on two random ramets within the collar. LDMC was measured from two leaf samples taken from two different ramets. If only one ramet of a species was present within the collar, height was measured only once, and two leaf samples were taken from that one ramet. The leaf samples were taken at the time of community surveys, put in re-sealable plastic bags with moist paper towels, and transported to the lab to be stored at 4□ for up to three days, before weighing for fresh mass. The leaves were then dried at 70□ for 48 h and weighed for dry mass. A precision scale with a resolution of 0.001 g was used for weighing. LDMC is dry mass divided by fresh mass, and is thus unitless. Location-specific trait values for each species were quantified as the average of the two individual trait values.

As a measure of functional composition, we used community weighted means (CWM) of these two traits, which have been shown to correlate with environmental conditions and ecosystem functioning (Garnier *et al.*, 2004). We chose coefficient of variation (CV, standard deviation/mean) as the measure of functional diversity. Many traits have a log-normal distribution, meaning that natural variation within a community increases with average trait values (Bjorkman *et al.*, 2018b). The CV represents trait variation in relation to that which would be expected for a given CWM value, and can be thought of as normalized functional variation in relation to functional composition. In the analysis, we refer to these variables as height, LDMC, CV_{height} and CV_{LDMC}.

CO_2 flux data

We measured CO_2 exchange in 200 locations using a static, non-steady state non-flow-through system (Livingston & Hutchinson, 1995) composed of a transparent acrylic chamber (20 cm diameter, 25 cm height). The chamber included a small ventilator, a carbon dioxide probe GMP343 (A1A1N0N0N0A model; CO_2 range 0–1000 ppm, ± 3 ppm + 1%), an air humidity and temperature probe HMP75 (temperature range between -20 and 60°C, relative

humidity range 0–100 %; temperature accuracy at 20°C ± 0.2°C, relative humidity accuracy between -20 and + 40°C ± (1.0 + 0.008 * relative humidity reading)), and a measurement indicator MI70 (Vaisala, Vantaa, Finland). In the chamber, CO_2 concentration, air temperature and relative humidity were recorded at 5-s intervals for 90 s. Concentrations of CO_2 were already corrected for atmospheric pressure and relative humidity during the measurements. PAR was logged manually at 10-s intervals during the same period using a MQ-200 quantum sensor with a hand-held meter (Apogee Instruments, Inc, USA). MQ-200 measures PAR at a spectral range from 410 to 655 nm.

Steel soil collars (21 cm in diameter and 6–7 cm in height) were inserted in the soil at least 24 h before the measurements to avoid potential CO_2 flush from soil that may arise from the disturbance caused by the installation of the collars. The soils in the study area are relatively rocky and have long horizontal roots growing through them, thus our collars were embedded only *ca*. 2 cm into the soil. To guarantee an air-tight seal, we sealed the edges of the collar using inert quartz sand. The chamber was placed on top of the collar and ventilated after each measurement. We progressively decreased the light intensity of NEE measurements from ambient conditions to *ca*. 80%, 50% and 30% PPFD by shading the chamber with layers of white mosquito net (n = 7–10). ER was measured in dark conditions (0 PPFD), which were obtained by covering the chamber with a space blanket (n = 3). To measure SR, all above-ground vascular plant biomass was clipped. The clipping was done ≥24 h before the measurements to avoid disturbance. We conducted three SR measurements in dark conditions in each plot. The soil CO_2 emissions consist partially of moss and lichen respiration, as we were not able to remove entirely all miniature cryptogams on the soil due to their tight integration with the soil particles. Each plot was visited twice at midday during the peak season in 2017. During the first time, plots were visited to measure NEE and ER between the 26th of June and 27th of July, and during the second time, plots were visited to measure SR between the 7th and 15th of August.

Before flux calculations, we deleted the first and last 5 s of the measurements to remove potentially disturbed observations. Thus, the final measurement period was 80 s for each plot. Fluxes (F) were calculated following Kulmala *et al.*, 2004:

$$F = \frac{\Delta C}{\Delta t}\frac{M}{Vmol}\frac{Vc}{Ac} \quad \text{(Eqn 1)}$$

where $\frac{\Delta C}{\Delta t}$ is the change in CO_2 concentration in time, M is the molecular mass of CO_2 (44.01 g mol^{-1}), Vmol the molar volume ($22.4*10^{-3}$ m^3 mol^{-1}) and Vc the volume of the air space in the chamber, and A the area of the collar. The flux unit was µmol m^{-2} s^{-1}.

Carbon stock data

We measured the depth of the soil organic and mineral layers from three points on each plot using a metal probe. In the analyses, we used the mean value of the three point measurements to represent the organic and mineral layer depths in each plot. We collected samples of roughly 1 dl from the soil organic and mineral layers with metal soil core cylinders (4 to 6 cm in diameter, 5 to 7 cm height). The organic samples were collected from the top soil, and mineral samples directly below the organic layer. The soil samples were taken *ca*. 2 m from the central plot of the moisture measurement scheme to avoid perturbation, on the 1st to 31st of August 2016 and 2017. The laboratory analyses were carried out in the Laboratory of Geosciences and Geography and Laboratory of Forest Sciences (University of Helsinki). We used a freeze-drying method to remove moisture from the samples. Bulk density (kg m^{-3}) was estimated by dividing the dry weight by the sample volume. Total carbon content (C%) analyses were done using either Vario Elementar Micro cube or Vario Elemantar Max - analyzer (Elementar Analysensysteme GmbH, Germany). Before C% analysis, mineral samples were sieved through a 2 mm plastic sieve. Organic samples were homogenized by hammering the material into smaller pieces.

SOC for organic and mineral layer was estimated using Equation 2:

$$SOC = C\%/100\,\% \times bulkdensity(kgm^{-3}) \times layerdepth(m) \quad \text{(Eqn 2)}$$

We had the C% and bulk density information for all organic samples, but we had 54 mineral soil samples with C% and 70 mineral samples with bulk density estimates from the study area. We used the median of these samples (3% for C% and 830 kg m^{-3} for bulk density) for the carbon stock estimates in all mineral layers, but the mineral layer depth varied across the sites. We consider this reliable due to the relatively low variability in mineral soil C% (0.4–6.5%) and bulk density (470–1400 kg m^{-3}). In some plots, we used soil organic matter content (SOM%) instead of C%. For more details, see Supporting Information, Methods S2.

Finally, organic and mineral layer stocks were summed together to calculate the total SOC stock. Plots with no soil were excluded from the analysis.

Above-ground vascular plant biomass was collected between the 1st and 10th of August from the collars. Biomass samples were oven-dried at 70°C for 48 h and weighed after drying. Above-ground carbon stocks (AGC) were estimated by multiplying the total biomass by 0.475 (Schlesinger, 1991). In the analysis, we refer to these variables as SOC and AGC.

Light response model and flux normalization

All models were run in R version 3.5.3 with the package *brms* version 2.8.0 (Bürkner, 2018), which is an interface to the Bayesian modelling platform Stan (Carpenter *et al.*, 2017). We fitted plot-specific light-response curves using the Michaelis-Menten equation in a non-linear hierarchical Bayesian model. The intercept term (dark respiration) was fitted with an exponential temperature response. For a full description of the model, see Supporting Information, Methods S3.

We used this model to predict the rate of NEE at dark (0 PPFD) and average light (600 PPFD) conditions, and a temperature of 20□ at each plot. We refer to the flux normalized to dark conditions as ecosystem respiration (ER). We then subtracted ER from the NEE normalized to average light conditions to arrive at an estimate of normalized GPP.

We also used this model together with PAR and temperature logger data to simulate plot-specific NEE with 10 minute intervals for the 30 day time period between the 8th of July and 7th of August 2017. Temperature measurements were first interpolated from 2–4 h to 10 minute resolution. We summed the predictions to create an estimate of peak-season CO_2 budget.

Soil respiration was normalized to 20□ with a Bayesian linear mixed model. The model included a plot-specific random intercept and a linear temperature response. All priors were left as the *brms* defaults. We refer to this variable hereafter as SR.

GPP and ER were calculated for all plots from which CO_2 measurements were taken (n = 200). Some of the steel collars were displaced between measurements of NEE and SR, thus SR was only measured in 192 plots. Peak-season CO_2 budget was calculated for all plots in which CO_2 fluxes were measured and were also continuously monitored for air temperature (n = 103). GPP, ER, and SR are always shown with positive signs. Positive numbers for NEE and CO_2 budget indicate net CO_2 gain to the ecosystem (i.e. CO_2 sink) and negative numbers indicate net CO_2 loss to the atmosphere (i.e. CO_2 source).

Hierarchical model of tundra carbon cycling

We built a hierarchical model of tundra carbon cycling by combining five submodels. The submodels describe 1) environmental effects on trait composition and diversity (n = 87), 2) trait effects on CO_2 fluxes (GPP, ER, SR, n = 129), 3) trait effects on above-ground carbon stocks (n = 134), 4) trait effects on soil organic carbon stocks (n = 129), and 5) the sensitivity of peak-season CO_2 budget to photosynthesis and respiration (n = 102) (Fig. 2). The sample sizes of these models differed, because different variables were measured with different intensity. All response variables were modelled with first order linear regression. Plant height, CO_2 fluxes, and carbon stock variables were $\log_e$-transformed before analyses to satisfy the assumption of homoscedasticity. When a submodel had more than one response variable, we also modelled residual correlations among the response variables. For these models, priors were left as the *brms* default weakly informative priors. All models were fitted with four MCMC chains of 2000 iterations. The first 1000 samples of each chain were discarded as warmup, leaving 4000 MCMC samples of each parameter of each model.

Our hierarchical model only considered the indirect, trait-mediated effects of environmental conditions on carbon cycling. To see if the carbon-cycling submodels should include the direct effect of environmental conditions, we compared the predictive accuracy of models with direct and indirect environmental effects against those with indirect effects only using pareto-smoothed importance sampling leave-one-out cross-validation (Vehtari *et al.*, 2017), using the R-package *loo* version 2.1.0 (Vehtari *et al.*, 2019). Predictive accuracy was measured as expected log pointwise predictive density (ELPD). The models in this comparison were fitted to a common dataset, where none of the variables had missing observations (n = 80).

We used the carbon cycling model to simulate warming effects on ecosystem capacity to sequester carbon via changes in plant community functional composition and diversity. We predicted the peak-season CO_2 budget for median environmental conditions, a winter warming scenario (+1 February soil), a summer warming scenario (+1 July air temperature), and a combination of the two warming scenarios. For the scenarios with summer warming, we ran the simulations with and without direct temperature effects on summer respiration. Direct temperature effects were included in the models by multiplying predicted ER by the exponential of the temperature sensitivity parameter ($\beta_{Temperature}$, Eqn S2) from the previously fitted light-response model. We did not take into account residual uncertainty in the predictions. We propagated uncertainty by evenly sampling 500 predictions from the posterior distribution of each submodel, and used these values as the explanatory variables in the next model. Finally, we also thinned the predictions from the last model to 500 samples. For each scenario, we calculated the probability of the modelled ecosystem to be a net CO_2 sink.

Results

Light response model

The light response model used to calculate the normalized carbon flux variables seemed to converge; no MCMC chains showed erratic behaviour under visual inspection, and rank-normalized potential scale reduction factors for all parameters stayed below 1.01. Visual inspection of the posterior predictive distribution showed a very good fit to the data, also evidenced by a Bayesian R^2 (Gelman *et al.*, 2019) of 0.95.

Abiotic versus plant functional trait controls on carbon cycling

Models with only trait-related covariates predicted carbon cycling as accurately – or even more accurately – than models with both environmental and trait covariates (Fig. 3). By the principle of parsimony, we therefore focus our analysis on the simpler models.

Environmental controls on traits

Environmental conditions were better predictors of functional composition than of functional diversity. Vegetation height responded positively to both summer and winter temperatures (Figs. 4a, 5). There was less certainty about the effect of soil resources on vegetation height,

but the link seemed to be negative with a posterior probability of 96% (Supporting Information Fig. S1). LDMC was negatively associated with soil resources and winter temperatures (Fig. 4a).

The only statistically significant ($\alpha = 0.05$) environment–functional diversity connection was the positive link between February soil temperatures and CV_{LDMC}. The residual correlation between LDMC and CV_{Height} was negative ($\rho = -0.26$, CI = -0.46–-0.05). No other residual correlations were found among trait variables. Bayesian R^2s for the models explaining vegetation height, LDMC, CV_{Height} and CV_{LDMC} were 0.27, 0.41, 0.07, and 0.14, respectively.

Trait controls on CO_2 fluxes and carbon stocks

GPP, ER and SR had very similar responses to plant community functional composition and diversity. All fluxes responded positively to vegetation height and CV_{LDMC}, and negatively to LDMC (Figs. 4b, 5), although the link between LDMC and ER was negative with only 83% probability (Supporting Information, Fig. S2). Residual correlations between log-transformed flux pairs GPP-ER, GPP-SR, and ER-SR were 0.6, 0.3, and 0.5, respectively. Bayesian R^2s for the models explaining GPP, ER and SR were 0.43, 0.40 and 0.36, respectively.

AGC was positively related to vegetation height, LDMC, and CV_{Height} (Figs. 4c, 5, Supporting Information Fig. S3). SOC was positively related to CV_{LDMC} (Fig. 4d, Supporting Information Fig. S4). LDMC and SOC had positive residual correlations with a 97.5% probability. Bayesian R^2s for the models explaining AGC and SOC were 0.39 and 0.15, respectively.

CO_2 budget sensitivity to warming

The simulated peak-season CO_2 budget was 1.4 times more sensitive to changes in ER than in GPP (Fig. 4d). Fluctuating light and temperature levels and the nonlinear light response curve did not cause major nonlinearities in the determination of the budget, indicated by the 0.98 R^2 of the linear model. The expected peak-season CO_2 budget was positively affected by the functional changes brought about by simulated summer and winter warming, even when the direct effects of respiration were taken into account (Fig. 6). The probability of an ecosystem patch being a summer net CO_2 sink grew in all but one scenario. In the simulation with

summer warming and a direct temperature effect, the probability of being a sink fell by one percentage point.

Discussion

Arctic vegetation is being reshuffled at unprecedented speed (Post *et al.*, 2009), both in predictable and surprising ways (Jia *et al.*, 2003, Phoenix & Bjerke, 2016). Thus, it is imperative that we form a solid understanding of the causal forces shaping Arctic ecosystems and their functioning. Here, by using a hierarchical modeling framework, we provide new insights into the relative roles of environmental conditions and plant functional traits in determining CO_2 fluxes and carbon stocks in the tundra. While instantaneous conditions do affect CO_2 fluxes, the main effects of average surface temperatures and soil resource availability on carbon cycling are mediated through their effects on plant community functional composition. A functional trait-based approach proved especially informative, since we were able to partition the effects of vegetation composition and diversity on carbon cycling to size and resource use strategy-related components. The axes of plant functional trait variation identified in recent years (Díaz *et al.*, 2016; Bruelheide *et al.*, 2018) have clearly separate effects on tundra carbon cycling. Thus, traits can inform us about the impacts of global change and vegetation shift on carbon cycling and resulting climate feedbacks.

Plant community functional composition regulates fine-scale carbon cycling

Plant size had a strong and positive relationship with all fluxes and pools except for soil organic carbon stocks. Evidence suggests that plant size is increasing around the Arctic in response to climate change. Sometimes this is in part due to “shrubification”, or the increases in the biomass, cover, and abundance of woody species (Myers-Smith *et al.*, 2011), but also other large species (Bjorkman *et al.*, 2018a). From our results it follows that the documented trait changes around the tundra have already caused large shifts in the functioning of Arctic ecosystems.

Leaf economic spectrum effects on carbon cycling were more variable. Our study supports the well-established strong positive relationship between faster economic traits and photosynthesis (Williams *et al.*, 2006; Street *et al.*, 2007; Shaver *et al.*, 2007), but suggests

that the connection to ecosystem respiration is not as strong. The relationship between ecosystem respiration and traits is more complicated due to the various sources of ecosystem respiration (above-ground plant tissues, roots, symbionts and heterotrophs) which all have different drivers (Barba *et al.*, 2017). The positive effect of leaf economics on soil respiration was stronger and more certain than on ecosystem respiration. We speculate that there are three potential reasons for this. First, faster growing plants often produce more litter that is rich in nutrients and more easily broken down by soil microbes, resulting in higher soil respiration rates (Cornwell *et al.*, 2008; Freschet *et al.*, 2012). Second, faster plants produce more root exudates, which are, together with root respiration, suggested to be a main source of soil respiration in the tundra (Illeris *et al.*, 2003). Third, plants with high leaf nutrient concentrations also have high nutrient concentrations in the roots, as suggested by whole-plant economic spectrum (Freschet *et al.*, 2010), which might also accelerate soil respiration by facilitating, for example, root respiration (Jia *et al.*, 2013). Thus, there are complex background processes that could be associated with the relationships that we have observed.

Although above-ground traits were linked to soil respiration, they were poorly linked with soil organic carbon stocks. Moreover, a large part of variation in soil organic carbon stocks remained unexplained. Soil organic carbon stocks were weakly related to traits because they are a result of carbon inputs from above- and below-ground plant tissues, outputs from ecosystem and soil respiration, and lateral transport, which all respond differently to trait variation. Trait effects on soil organic carbon stocks are also more indirect (e.g. via litter decomposition and accumulation) compared to, for example, the relationship between leaf economics and photosynthesis (De Deyn *et al.*, 2008). In addition to above-ground vascular plant traits, soil organic carbon stocks could be explained by the traits of mosses, which can play an important role in wetter landscape positions (Douma *et al.*, 2007), or litter and root traits which are more directly linked with soil organic carbon stocks (Orwin *et al.*, 2010). Soil organic carbon stocks are also likely influenced by additional abiotic drivers, such as aeolian and fluvial transportation of litter (Klaminder *et al.*, 2009), or soil development and carbon accumulation in the past (Palmtag *et al.*, 2015).

Functional diversity increases CO_2 fluxes and carbon stocks

All fluxes and soil organic carbon stocks responded positively to the functional diversity of leaf economics, but not to the diversity of plant size. Thus, within-community variability on

the slow-fast strategy axis increased ecosystem functioning, supporting the niche complementarity hypothesis (Tilman *et al.*, 1997), but size variation did not. There are several mechanisms for how soil organic carbon stocks could increase with plant functional diversity. One such mechanism is that increased productivity could lead to higher litter inputs from leaves and roots (DeMarco *et al.*, 2014). Since leaf economic diversity did not increase above-ground carbon stocks, our interpretation is that the positive diversity effect on soil organic carbon stocks is probably due to increased root litter production, indicative of higher total investments in acquiring below-ground resources. These observations would be consistent with more efficient partitioning of below-ground resources, which would also explain the positive effects of leaf economic diversity on CO_2 fluxes.

Functional diversity of plant size was positively associated with above-ground carbon stocks, indicating that multi-layered vegetation stores more carbon compared to less structurally diverse plant communities. Similar effects of size-related trait diversity on above-ground biomass have been reported for German semi-natural grasslands (Schumacher & Roscher, 2009). On the other hand, Conti & Díaz (2013) reported a negative correlation between structural diversity and above-ground carbon stocks in Argentinian forests, but note that this is probably due to confounding factors. Our results provide strong evidence that structurally layered tundra communities do indeed contain more carbon than vertically homogeneous vegetation patches, because we modelled the effects of structural and resource-use trait diversities separately, and because we controlled for the direct effects of functional composition in constructing our diversity measures.

Effects of warmer temperatures on peak-season CO_2 budget

Simulated warming increased the capacity of ecosystems to sequester carbon during peak growing season. This held true for both for summer air and winter soil temperatures. These effects manifested through different mechanisms: summer warming increased photosynthesis by increasing plant size, while winter warming both increased plant size and accelerated leaf economics. This demonstrates how environmental conditions outside the growing season are important for understanding changes in high-latitude ecosystem functioning (Happonen *et al.*, 2019).

Our results suggest that +1 higher summer air temperatures increase summer ecosystem respiration by *ca.* 3%. Including this direct temperature effect on peak-season CO_2 budget did not reverse the expected summer warming effects on the budget, but it did slightly increase the probability of vegetation turning into a CO_2 source. Results from other parts of the tundra have shown that short-term warming can in fact decrease net carbon uptake during the growing season by increasing respiration more than photosynthesis (Biasi *et al.*, 2008; Parmentier *et al.*, 2011). Based on our results, this is also true in Scandinavian mountain tundra, but the long-term effects on peak-season CO_2 budget are more likely to be positive due to warming effects on plant functional traits. These positive indirect effects are not certain to be realized, however. For example, reindeer grazing has been shown to buffer tundra communities against the expansion of taller species (Kaarlejärvi *et al.*, 2013; Vuorinen *et al.*, 2017). Even without biotic buffering, dispersal limitation and other inertia in the population dynamics of long-lived tundra species can cause time lags in vegetation transitions (Alexander *et al.*, 2018), whereas accelerated respiration in response to temperature increase is more or less immediate. Taken together with the fact that respiratory carbon losses are bound to increase also beyond the peak growing season, and that the effects of climate change on winter soil temperatures are modulated by changes in snow cover duration and depth (Nobrega & Grogan, 2007), our results cannot be interpreted to mean that future warming will increase the annual carbon sink of the tundra.

Conclusions

We found that in a tundra landscape, fine-scale carbon cycling was parsimoniously explained by plant community functional composition and diversity, and that long-term environmental conditions had only indirect effects. Average plant size was the strongest predictor of most carbon cycling variables, but leaf economic diversity mattered the most for soil organic carbon stocks. Plant size increased CO_2 fluxes and above-ground carbon stocks, whereas fast leaf economics were associated with higher CO_2 fluxes and lower above-ground carbon stocks. All carbon cycling variables were positively affected by the diversity of some functional trait. Both warmer summer air and winter soil temperatures would lead to functional changes in plant communities that would enhance carbon uptake during the peak season. Our findings are a step forward in forming an integrated view on the causes and ecosystem consequences of climate change-related vegetation transitions in the tundra.

Acknowledgements

The authors thank Juha Aalto, Liangzhi Chen, Elisa Hanhirova, Pinja-Liina Jalkanen, Ari-Pekka Jokinen, Tytti Jussila, Arttu Kivimäki, Panu Lammi, Meri Lindholm, Mitro Müller, Tiia Määttä, Aino-Maija Määttänen, Annina Niskanen, Nina Nordblad, Helena Rautakoski, Henri Riihimäki, Tuuli Rissanen, Sakari Sarjakoski, Outi Seppälä, Vilna Tyystjärvi, Akseli Toikka, and the Arctic Microbial Ecology group at the University of Helsinki for their field and laboratory work, and the staff of the Kilpisjärvi Biological Station for their help. KH was funded by the Doctoral Programme in Wildlife Biology Research at the University of Helsinki. A-MV was funded by Societas pro Fauna et Flora Fennica, Otto Malm foundation, Nordenskiöld-samfundet, Alfred Kordelin foundation, Finnish Cultural Foundation, Academy of Finland (project no. 286950), and Väisälä fund. JK was funded by the Doctoral Programme in Geosciences at the University of Helsinki, Maa- ja vesitekniikan tuki ry. and Tiina and Antti Herlin Foundation. The authors acknowledge funding from the Academy of Finland (project 286950).

Author contributions

KH, AMV and ML conceived the research. KH, AMV, JK and PN collected the field data. KH and AMV preprocessed the data. KH, with support from AMV, analysed the data. KH and AMV, with the support of all co-authors, wrote the paper.

Data availability

The data and analysis code used in this study will be deposited to Zenodo upon publication.

References

Adler PB, Salguero-Gómez R, Compagnoni A, Hsu JS, Ray-Mukherjee J, Mbeau-Ache C, Franco M. **2014**. Functional traits explain variation in plant life history strategies. *Proceedings of the National Academy of Sciences* **111**: 740–745.

Alexander JM, Chalmandrier L, Lenoir J, Burgess TI, Essl F, Haider S, Kueffer C, McDougall K, Milbau A, Nuñez MA, *et al.* 2018. Lags in the response of mountain plant communities to climate change. *Global Change Biology* **24**: 563–579.

Barba J, Cueva A, Bahn M, Barron-Gafford GA, Bond-Lamberty B, Hanson PJ, Jaimes A, Kulmala L, Pumpanen J, Scott RL, *et al.* 2017. Comparing ecosystem and soil respiration: Review and key challenges of tower-based and soil measurements. *Agricultural and Forest Meteorology* **249**: 434–443.

Bar-On YM, Phillips R, Milo R. **2018**. The biomass distribution on Earth. *Proceedings of*

the National Academy of Sciences **115**: 6506–6511.
Bates D, Mächler M, Bolker B, Walker S. **2015**. Fitting Linear Mixed-Effects Models Using lme4. *Journal of Statistical Software, Articles* **67**: 1–48.
Biasi C, Meyer H, Rusalimova O, Hämmerle R, Kaiser C, Baranyi C, Daims H, Lashchinsky N, Barsukov P, Richter A. **2008**. Initial effects of experimental warming on carbon exchange rates, plant growth and microbial dynamics of a lichen-rich dwarf shrub tundra in Siberia. *Plant and Soil* **307**: 191–205.
Bjorkman AD, Myers-Smith IH, Elmendorf SC, Normand S, Rüger N, Beck PSA, Blach-Overgaard A, Blok D, Cornelissen JHC, Forbes BC, *et al.* 2018a. Plant functional trait change across a warming tundra biome. *Nature* **562**: 57.
Bjorkman AD, Myers□Smith IH, Elmendorf SC, Normand S, Thomas HJD, Alatalo JM, Alexander H, Anadon□Rosell A, Angers□Blondin S, Bai Y, *et al.* 2018b. Tundra Trait Team: A database of plant traits spanning the tundra biome. *Global Ecology and Biogeography* **27**: 1402–1411.
Bruelheide H, Dengler J, Purschke O, Lenoir J, Jiménez-Alfaro B, Hennekens SM, Botta-Dukát Z, Chytrý M, Field R, Jansen F, *et al.* 2018. Global trait–environment relationships of plant communities. *Nature Ecology & Evolution* **2**: 1906.
Bürkner P-C. **2018**. Advanced Bayesian Multilevel Modeling with the R Package brms. *The R Journal* **10**: 395–411.
Cadotte MW, Carscadden K, Mirotchnick N. **2011**. Beyond species: functional diversity and the maintenance of ecological processes and services. *Journal of Applied Ecology* **48**: 1079–1087.
Cahoon SMP, Sullivan PF, Shaver GR, Welker JM, Post E. **2012**. Interactions among shrub cover and the soil microclimate may determine future Arctic carbon budgets. *Ecology Letters* **15**: 1415–1422.
Carpenter B, Gelman A, Hoffman MD, Lee D, Goodrich B, Betancourt M, Brubaker M, Guo J, Li P, Riddell A. **2017**. Stan: A Probabilistic Programming Language. *Journal of Statistical Software* **76**: 1–32.
Conti G, Díaz S. **2013**. Plant functional diversity and carbon storage – an empirical test in semi-arid forest ecosystems. *Journal of Ecology* **101**: 18–28.
Cornwell WK, Cornelissen JHC, Amatangelo K, Dorrepaal E, Eviner VT, Godoy O, Hobbie SE, Hoorens B, Kurokawa H, Pérez-Harguindeguy N, *et al.* 2008. Plant species traits are the predominant control on litter decomposition rates within biomes worldwide. *Ecology Letters* **11**: 1065–1071.
DeMarco J, Mack MC, Bret-Harte MS, Burton M, Shaver GR. **2014**. Long-term experimental warming and nutrient additions increase productivity in tall deciduous shrub tundra. *Ecosphere* **5**: 72.
Díaz S, Hodgson JG, Thompson K, Cabido M, Cornelissen JHC, Jalili A, Montserrat□Martí G, Grime JP, Zarrinkamar F, Asri Y, *et al.* 2004. The plant traits that drive ecosystems: Evidence from three continents. *Journal of Vegetation Science* **15**: 295–304.
Díaz S, Kattge J, Cornelissen JHC, Wright IJ, Lavorel S, Dray S, Reu B, Kleyer M, Wirth C, Colin Prentice I, *et al.* 2016. The global spectrum of plant form and function. *Nature* **529**: 167.
Díaz S, Lavorel S, Bello F de, Quétier F, Grigulis K, Robson TM. **2007**. Incorporating plant functional diversity effects in ecosystem service assessments. *Proceedings of the National Academy of Sciences* **104**: 20684–20689.
Douma JC, Van Wijk MT, Lang SI, Shaver GR. **2007**. The contribution of mosses to the carbon and water exchange of arctic ecosystems: quantification and relationships with system properties. *Plant Cell and Environment* **30**: 1205–1215.

Duffy JE, Godwin CM, Cardinale BJ. **2017**. Biodiversity effects in the wild are common and as strong as key drivers of productivity. *Nature* **549**: 261.

Finnish Meteorological Institute. **2019a**. Daily climate observations. Enontekiö Kilpisjärvi Saana.

Finnish Meteorological Institute. **2019b**. Daily climate observations. Enontekiö Kilpisjärvi kyläkeskus.

Freschet GT, Aerts R, Cornelissen JHC. **2012**. A plant economics spectrum of litter decomposability. *Functional Ecology* **26**: 56–65.

Freschet G, Cornelissen J, Logtestijn R, Aerts R. **2010**. Evidence of the 'Plant Economics Spectrum' in a Subarctic Flora. *Journal of Ecology* **98**: 362–373.

Garnier E, Cortez J, Billès G, Navas M-L, Roumet C, Debussche M, Laurent G, Blanchard A, Aubry D, Bellmann A, *et al.* 2004. Plant Functional Markers Capture Ecosystem Properties During Secondary Succession. *Ecology* **85**: 2630–2637.

Gelman A, Goodrich B, Gabry J, Vehtari A. **2019**. R-squared for Bayesian Regression Models. *The American Statistician* **73**: 307–309.

Grime JP. **1998**. Benefits of plant diversity to ecosystems: immediate, filter and founder effects. *Journal of Ecology* **86**: 902–910.

Happonen K, Aalto J, Kemppinen J, Niittynen P, Virkkala A-M, Luoto M. **2019**. Snow is an important control of plant community functional composition in oroarctic tundra. *Oecologia* **191:** 601.

Holland MM, Landrum L. **2015**. Factors affecting projected Arctic surface shortwave heating and albedo change in coupled climate models. *Philosophical Transactions of the Royal Society A: Mathematical, Physical and Engineering Sciences* **373**: 20140162.

Hugelius G, Strauss J, Zubrzycki S, Harden JW, Schuur EAG, Ping CL, Schirrmeister L, Grosse G, Michaelson GJ, Koven CD, *et al.* 2014. Estimated stocks of circumpolar permafrost carbon with quantified uncertainty ranges and identified data gaps. *Biogeosciences* **11**: 6573–6593.

Illeris L, Michelsen A, Jonasson S. **2003**. Soil plus root respiration and microbial biomass following water, nitrogen, and phosphorus application at a high arctic semi desert. *Biogeochemistry* **65**: 15–29.

ISO 10390. **2005**. Soil quality - Determination of pH.

Jia GJ, Epstein HE, Walker DA. **2003**. Greening of arctic Alaska, 1981–2001. *Geophysical Research Letters* **30**.

Jia S, McLaughlin NB, Gu J, Li X, Wang Z. **2013**. Relationships between root respiration rate and root morphology, chemistry and anatomy in Larix gmelinii and Fraxinus mandshurica. *Tree Physiology* **33**: 579–589.

Kaarlejärvi E, Eskelinen A, Olofsson J. **2013**. Herbivory prevents positive responses of lowland plants to warmer and more fertile conditions at high altitudes. *Functional Ecology* **27**: 1244–1253.

Kemppinen J, Niittynen P, Riihimäki H, Luoto M. **2018**. Modelling soil moisture in a high-latitude landscape using LiDAR and soil data. *Earth Surface Processes and Landforms* **43**: 1019–1031.

Kulmala L, Pumpanen J, Pohja T, Laakso H, Siivola E, Hari P, Vesala T. **2004**. A novel automatic chamber to measure soil CO2 efflux. *Report Series 109 of Finnish Association for Aerosol Research*.

Lavorel S, Garnier E. **2002**. Predicting changes in community composition and ecosystem functioning from plant traits: revisiting the Holy Grail. *Functional Ecology* **16**: 545–556.

Livingston GP, Hutchinson GL. **1995**. Enclosure-based measurement of trace gas exchange: applications and sources of error. In: Biogenic trace gases: Measuring emissions from soil and water. Oxford, United Kingdom: Blackwell Science, 14–51.

McGill BJ, Enquist BJ, Weiher E, Westoby M. **2006**. Rebuilding community ecology from functional traits. *Trends in Ecology & Evolution* **21**: 178–185.

Messier J, McGill BJ, Lechowicz MJ. **2010**. How do traits vary across ecological scales? A case for trait-based ecology. *Ecology Letters* **13**: 838–848.

Michaletz ST, Cheng D, Kerkhoff AJ, Enquist BJ. **2014**. Convergence of terrestrial plant production across global climate gradients. *Nature* **512**: 39–43.

Myers-Smith IH, Elmendorf SC, Beck PSAA, Wilmking M, Hallinger M, Blok D, Tape KD, Rayback SA, Macias-Fauria M, Forbes BC, *et al.* 2015. Climate sensitivity of shrub growth across the tundra biome. *NATURE CLIMATE CHANGE* **5**: 887–891.

Myers-Smith IH, Forbes BC, Wilmking M, Hallinger M, Lantz T, Blok D, Tape KD, Macias-Fauria M, Sass-Klaassen U, Lévesque E, *et al.* 2011. Shrub expansion in tundra ecosystems: dynamics, impacts and research priorities. *Environmental Research Letters* **6**: 045509.

Nobrega S, Grogan P. **2007**. Deeper Snow Enhances Winter Respiration from Both Plant-associated and Bulk Soil Carbon Pools in Birch Hummock Tundra. *Ecosystems* **10**: 419–431.

Orwin KH, Buckland SM, Johnson D, Turner BL, Smart S, Oakley S, Bardgett RD. **2010**. Linkages of plant traits to soil properties and the functioning of temperate grassland: Links of plant traits to soil properties. *Journal of Ecology* **98**: 1074–1083.

Palmtag J, Hugelius G, Lashchinskiy N, Tamstorf MP, Richter A, Elberling B, Kuhry P. **2015**. Storage, Landscape Distribution, and Burial History of Soil Organic Matter in Contrasting Areas of Continuous Permafrost. *Arctic, Antarctic, and Alpine Research* **47**: 71–88.

Parker TC, Subke JA, Wookey PA. **2015**. Rapid carbon turnover beneath shrub and tree vegetation is associated with low soil carbon stocks at a subarctic treeline. *Global Change Biology* **21**: 2070–2081.

Parmentier FJW, Molen MK van der, Huissteden J van, Karsanaev SA, Kononov AV, Suzdalov DA, Maximov TC, Dolman AJ. **2011**. Longer growing seasons do not increase net carbon uptake in the northeastern Siberian tundra. *Journal of Geophysical Research: Biogeosciences* **116**.

Phoenix GK, Bjerke JW. **2016**. Arctic browning: extreme events and trends reversing arctic greening. *Global Change Biology* **22**: 2960–2962.

Schlesinger WH. **1991**. *Biogeochemistry, an Analysis of Global Change*. New York, USA: Academic Press.

Schumacher J, Roscher C. **2009**. Differential effects of functional traits on aboveground biomass in semi natural grasslands. *Oikos* **118**: 1659–1668.

SFS. **1990**. 3008. Determination of total residue and total fixed residue in water, sludge and sediment.

Shaver GR, Billings WD, Chapin FS, Giblin AE, Nadelhoffer KJ, Oechel WC, Rastetter EB. **1992**. Global Change and the Carbon Balance of Arctic EcosystemsCarbon/nutrient interactions should act as major constraints on changes in global terrestrial carbon cycling. *BioScience* **42**: 433–441.

Shaver GR, Street LE, Rastetter EB, Van Wijk MT, Williams M. **2007**. Functional convergence in regulation of net CO_2 flux in heterogeneous tundra landscapes in Alaska and Sweden. *Journal of Ecology* **95**: 802–817.

Sørensen MV, Strimbeck R, Nystuen KO, Kapas RE, Enquist BJ, Graae BJ. **2017**. Draining the Pool? Carbon Storage and Fluxes in Three Alpine Plant Communities. *Ecosystems*: 1–15.

Steinbauer MJ, Grytnes J-A, Jurasinski G, Kulonen A, Lenoir J, Pauli H, Rixen C, Winkler M, Bardy-Durchhalter M, Barni E, *et al.* 2018. Accelerated increase in plant species richness on mountain summits is linked to warming. *Nature* **556**: 231.

Street LE, Shaver GR, Williams M, Van Wijk MT. **2007**. What is the relationship between changes in canopy leaf area and changes in photosynthetic CO2 flux in arctic ecosystems? *Journal of Ecology* **95**: 139–150.

Thomas HJD, Myers-Smith IH, Bjorkman AD, Elmendorf SC, Blok D, Cornelissen JHC, Forbes BC, Hollister RD, Normand S, Prevéy JS, *et al.* 2019. Traditional plant functional groups explain variation in economic but not size-related traits across the tundra biome. *Global Ecology and Biogeography* **28**: 78–95.

Tilman D, Isbell F, Cowles JM. **2014**. Biodiversity and Ecosystem Functioning. *Annual Review of Ecology, Evolution, and Systematics* **45**: 471–493.

Tilman D, Knops J, Wedin D, Richie M, Siemann E. **1997**. The Influence of Functional Diversity and Composition on Ecosystem Processes | Science. *Science* **277**: 1300–1302.

Vehtari A, Gabry J, Yao Y, Gelman A. **2019**. *loo: Efficient leave-one-out cross-validation and WAIC for Bayesian models*.

Vehtari A, Gelman A, Gabry J. **2017**. Practical Bayesian model evaluation using leave-one-out cross-validation and WAIC. *Statistics and Computing* **27**: 1413–1432.

Villéger S, Grenouillet G, Brosse S. **2013**. Decomposing functional β-diversity reveals that low functional β-diversity is driven by low functional turnover in European fish assemblages. *Global Ecology and Biogeography* **22**: 671–681.

Virkkala A-M, Virtanen T, Lehtonen A, Rinne J, Luoto M. **2018**. The current state of CO2 flux chamber studies in the Arctic tundra: A review. *Progress in Physical Geography: Earth and Environment* **42**: 162–184.

Vuorinen KEM, Oksanen L, Oksanen T, Pyykönen A, Olofsson J, Virtanen R. **2017**. Open tundra persist, but arctic features decline—Vegetation changes in the warming Fennoscandian tundra. *Global Change Biology* **23**: 3794–3807.

Williams M, Street LE, van Wijk MT, Shaver GR. **2006**. Identifying Differences in Carbon Exchange among Arctic Ecosystem Types. *Ecosystems* **9**: 288–304.

Wright IJ, Reich PB, Westoby M, Ackerly DD, Baruch Z, Bongers F, Cavender-Bares J, Chapin T, Cornelissen JHC, Diemer M, *et al.* 2004. The worldwide leaf economics spectrum. *Nature* **428**: 821.

Tables

Table 1. Glossary

Concept	**Definition**	**Variable used to represent the concept**	**Variable description**
Environmental drivers			
Soil resources	Substances that plants need in order to grow and reproduce, such as soil moisture and nutrients.	Soil resources	First axis from the Principal Component Analysis of soil moisture and soil organic layer pH
Summer temperature	Temperatures that the plants experience during the peak growing season.	Summer temperature	Average air temperatures in July from loggers
Winter temperature	Temperatures that the plants experience during the winter. This also correlates positively with snow depth.	Winter temperature	Average soil temperatures in February from loggers
Summer warming	Temperatures that the plants experience during the peak growing season in warmer conditions.	Summer warming	+1□ July air temperature warming scenario
Winter warming	Temperatures that the plants experience during the winter in warmer conditions.	Winter warming	+1□ February soil warming scenario
Plant functional traits			
Leaf economics	Describes differences between resource-acquisitive (fast) and resource-conservative (slow) plant communities. A measure of functional composition.	LDMC	Community weighted mean (CWM) of LDMC, calculated using vascular plant species point-intercept counts

Leaf economic diversity	Functional diversity on the leaf economics spectrum.	CV_{LDMC}	Coefficient of variation of LDMC
Plant size	Variation between plant communities caused by trade-offs between average investments in light competition, and photosynthesis and reproduction. A measure of functional composition.	Height	CWM of plant height
Plant size diversity	Functional diversity on the plant size spectrum.	CV_{height}	Coefficient of variation of height
Carbon cycling variables			
Photosynthesis	The process by which plants build carbohydrates from light and CO_2.	GPP	Gross primary productivity normalized at a common irradiance (600 PPFD, partly sunny conditions)
Ecosystem respiration	The process by which plants, soil animals and microbes convert sugars into energy, thus releasing CO_2 to the atmosphere.	ER	Ecosystem respiration normalized at a common air temperature (20°C, average air temperature)
Soil respiration	The sum of respiration of all heterotrophic organisms (decomposition by animals, fungi, and microbes) and root respiration.	SR	Soil respiration normalized at a common air temperature (20°C, average air temperature)
Peak-season CO_2 budget	CO_2 sequestration by gross primary productivity minus CO_2 release from ecosystem respiration accumulated over a certain period of time.	Peak-season CO_2 budget	GPP and ER were modeled over a 30-day period in July and August. Then, cumulative fluxes were calculated and NEE was estimated as GPP-ER.
Above-ground carbon stock	The carbon content in the living plant biomass.	AGC	Above-ground carbon stocks were estimated by multiplying the above-ground vascular plant

			biomass by 0.475.
Soil organic carbon stock	Soil organic carbon stocks in the entire soil horizon excluding roots.	SOC	Soil organic carbon stocks were estimated using the information of soil organic and mineral layer depth, bulk density, and soil carbon or soil organic matter content.

Figure legends

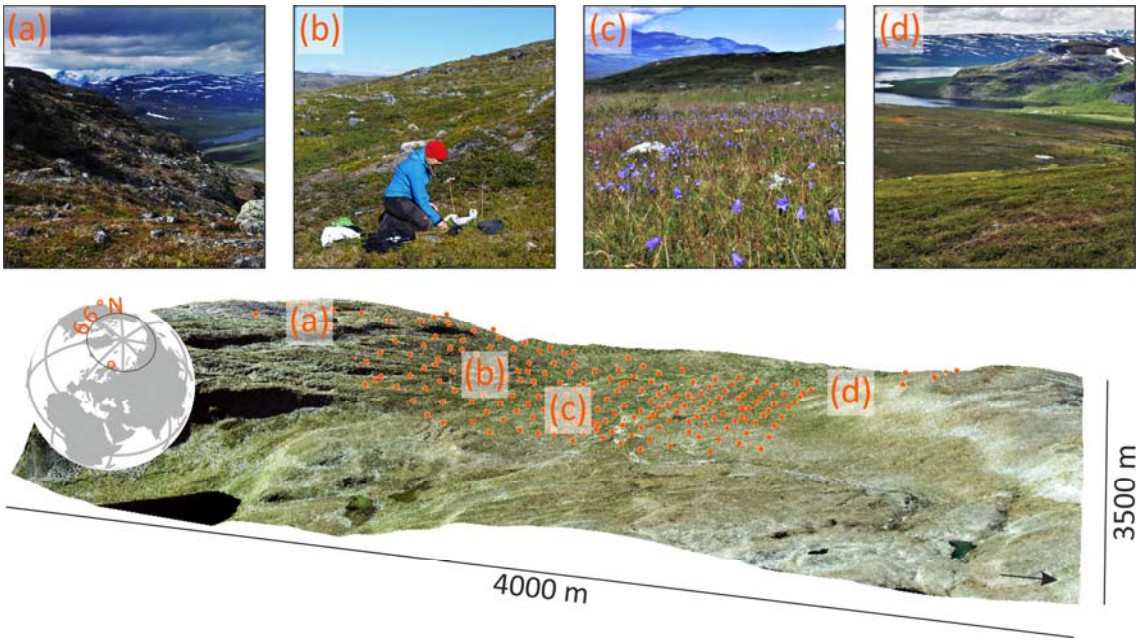

Figure 1. The sub-Arctic study site. The vegetation is heterogeneous, dominated by both deciduous (b: *Betula nana*, *Vaccinium myrtillus*) and evergreen (d: *Empetrum nigrum*) dwarf-shrub heaths. On the rocky slopes, the vegetation is sporadic (a), whereas lush meadows can be found in the valley bottom (c). Orange dots represent the 220 study locations, and the orange circle is the location of the study site. The orthophoto (0.5 m resolution) is provided by the National Land Survey of Finland (https://www.maanmittauslaitos.fi/en/maps-and-spatial-data/expert-users/product-descriptions/orthophotos, accessed on 2019-10-28.). Photographs by Julia Kemppinen.

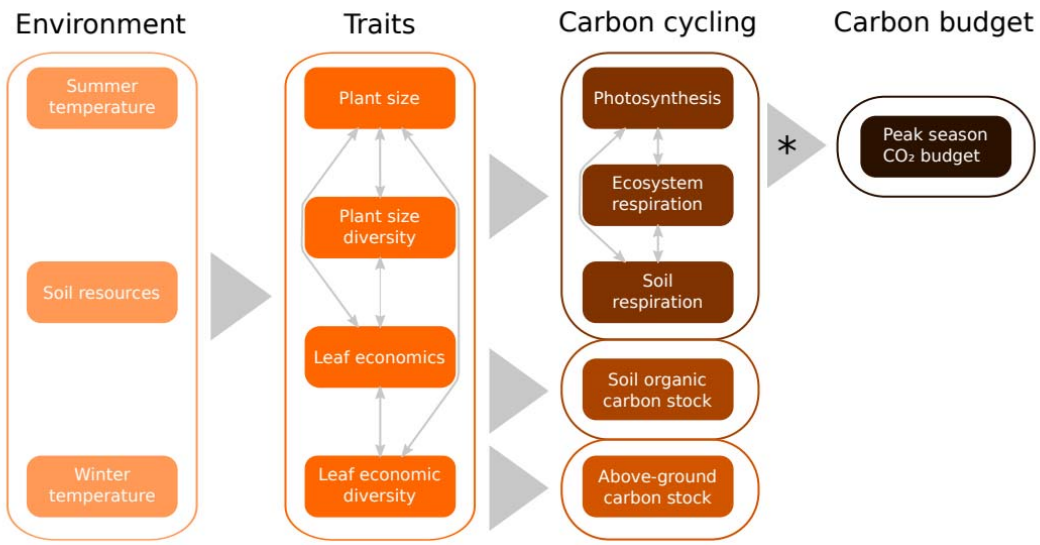

Figure 2. The theoretical framework that this study is based on, where traits act as mediating links between environmental conditions and carbon cycling. Large grey arrows represent the submodels, which describe environmental effects on trait composition and diversity, trait effects on CO_2 fluxes and carbon stocks, and the sensitivity of peak-season CO_2 budget to photosynthesis and respiration. When a submodel had more than one response variable, we also modelled residual correlations among the response variables, shown in thin grey arrows. Submodels used all explanatory variables (e.g. all carbon cycling submodels included all traits as covariates), except for the peak-season CO_2 budget model (marked with an asterisk), which omitted soil respiration, since it is a subcomponent of ecosystem respiration.

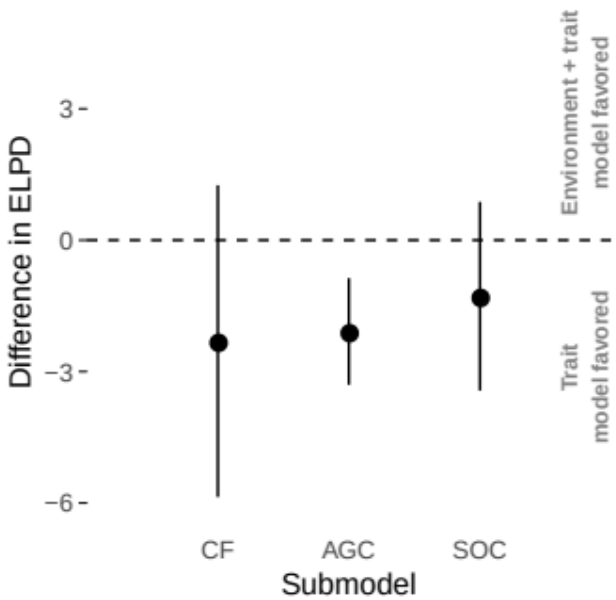

Figure 3. Predictive accuracy of CO_2 flux (CF), above-ground carbon stock (AGB) and soil organic carbon stock (SOC) models with traits and environmental variables or with traits alone as predictors. Predictive accuracy was measured as expected log pointwise predictive density (ELPD). The lines are 95% credible intervals around the point estimate.

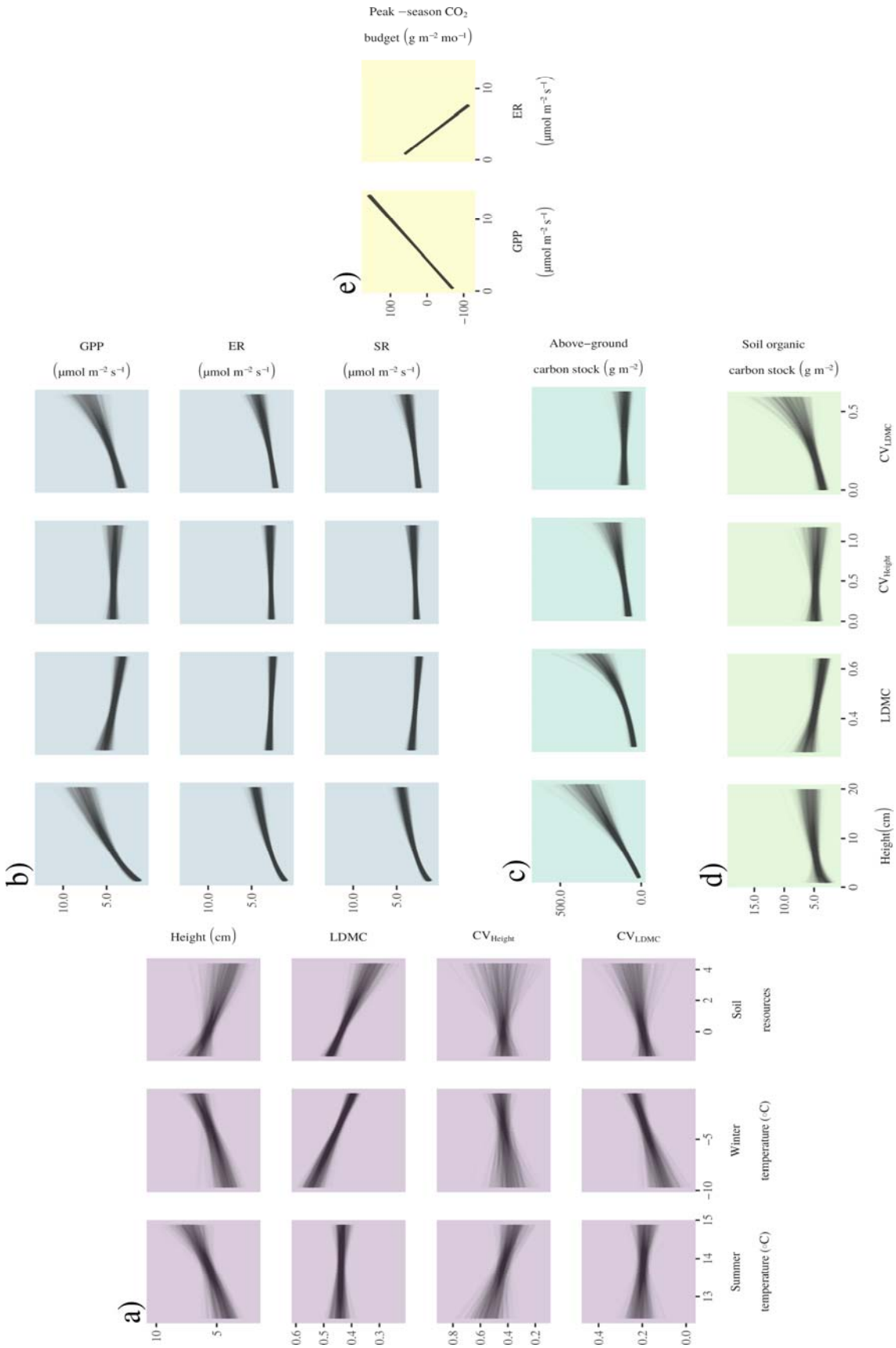
a)
Height (cm)
LDMC
CV_Height
CV_LDMC
Summer temperature (°C)
Winter temperature (°C)
Soil resources
b)
GPP (μmol m⁻² s⁻¹)
ER (μmol m⁻² s⁻¹)
SR (μmol m⁻² s⁻¹)
c)
Above-ground carbon stock (g m⁻²)
d)
Soil organic carbon stock (g m⁻²)
Height(cm)
LDMC
CV_Height
CV_LDMC
e)
Peak −season CO₂ budget (g m⁻² mo⁻¹)
GPP (μmol m⁻² s⁻¹)
ER (μmol m⁻² s⁻¹)

818

Figure 4. Modelled responses of a) plant community functional composition and diversity to the environment, b) CO_2 fluxes, c) above-ground carbon stocks and d) soil organic carbon stocks to plant community functional composition and diversity, and e) peak-season CO_2 budget to GPP and ER. Each panel uses 500 draws from the posterior distribution of the relevant parameter to simulate the marginal effect of one predictor when all other predictors are at their means. Height = community-weighted mean plant height, LDMC = community-weighted mean leaf dry matter content, CV_{height} = coefficient of variation of plant height, CV_{LDMC} = coefficient of variation of leaf dry matter content, Summer temperature = average July air temperature, Winter temperature= average February soil temperature, Soil resources = first principal component of soil moisture and pH, GPP = gross primary production normalized at a common irradiance (600 PPFD), ER = ecosystem respiration normalized at a common air temperature (20□), SR = soil respiration normalized at a common air temperature (20□), peak-season CO_2 budget = cumulative CO_2 balance over July.

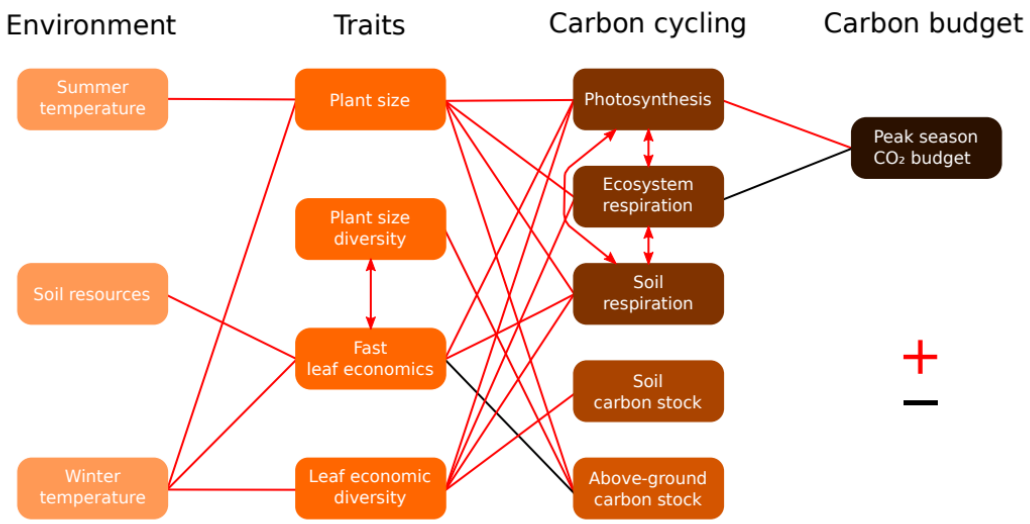

Figure 5. A dichotomized representation of the causal network implied by our hierarchical carbon cycling model. Lines show statistically significant relationships between the variables (α = 0.05, red = positive effect, black = negative effect). Variables on the left explain those on the right. Double-headed arrows represent residual correlations. Positive numbers for CO_2 budget indicate net CO_2 gain to the ecosystem (i.e. CO_2 sink). Low LDMC (leaf dry matter content) implies fast leaf economics, hence for ease of interpretation, all connections involving LDMC have been inverted for this figure (e.g. from negative to positive).

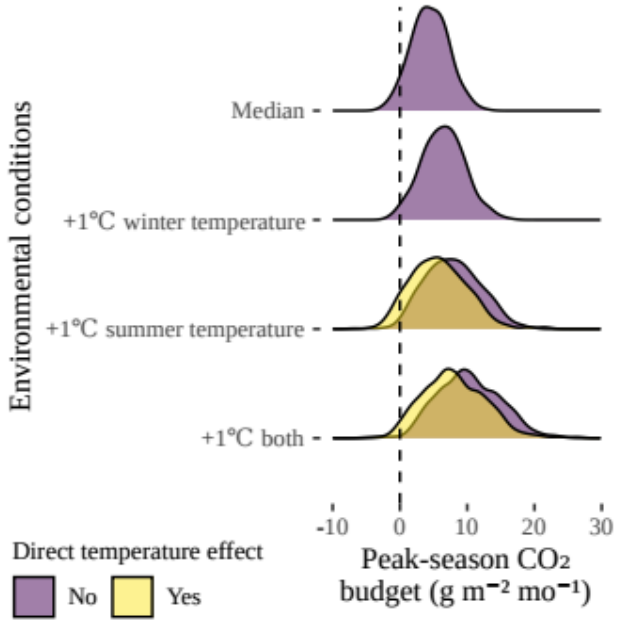

Figure 6. The effects of simulated warming on peak-season CO_2 budget with and without a direct temperature effect. Positive numbers for CO_2 budget indicate net CO_2 gain to the ecosystem (i.e. CO_2 sink).

Supporting information

Fig. S1 Kernel density plots of the posterior distributions of environmental effects on plant community functional composition and diversity. The lower x-axis is on the original scale, while the upper axis depicts the effects as standardized regression coefficients. The black line depicts the mean, the dark gray area around it ±1 SD, the lighter dark gray the 95% CI, and the lightest gray the rest of the distribution. LDMC = leaf dry matter content. CV = coefficient of variation.

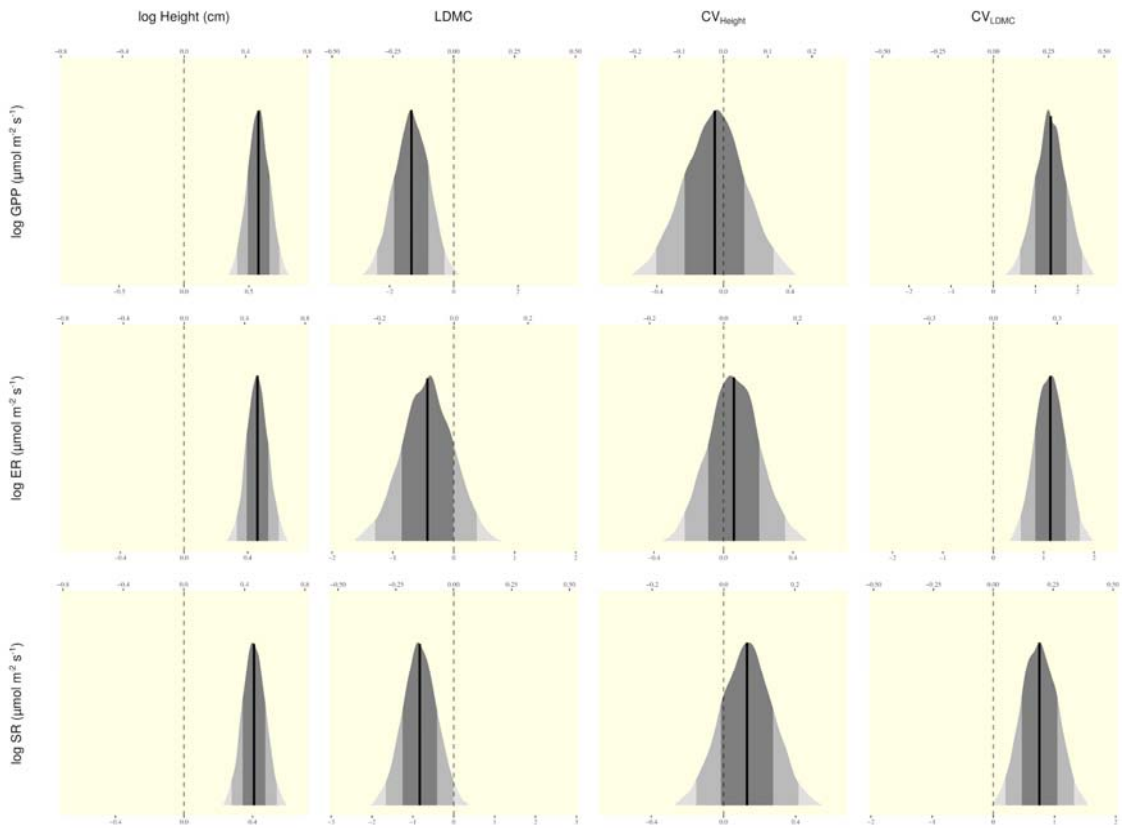

Fig. S2 Kernel density plots of the posterior distributions of trait effects on carbon fluxes. The lower x-axis is on the original scale, while the upper axis depicts the effects as standardized regression coefficients. The black line depicts the mean, the dark gray area around it ±1 SD, the lighter dark gray the 95% CI, and the lightest gray the rest of the distribution. GPP = normalized gross primary productivity. ER = normalized ecosystem respiration. SR = normalized soil respiration. LDMC = leaf dry matter content. CV = coefficient of variation.

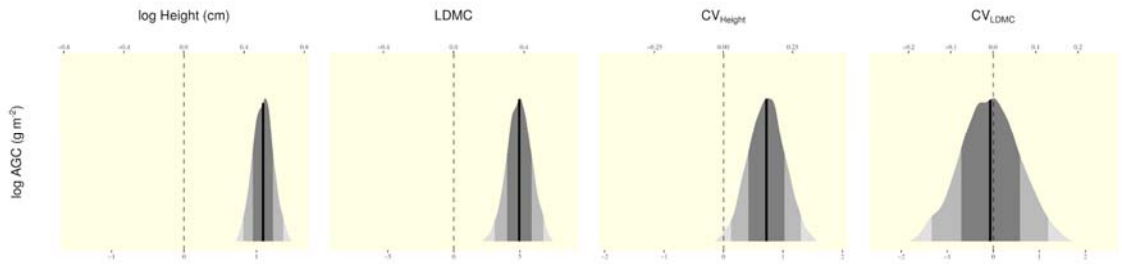

Fig. S3 Kernel density plots of the posterior distributions of trait effects above-ground carbon storage. The lower x-axis is on the original scale, while the upper axis depicts the effects as standardized regression coefficients. The black line depicts the mean, the dark gray area around it ±1 SD, the lighter dark gray the 95% CI, and the lightest gray the rest of the distribution. AGC = above-ground carbon stock. LDMC = leaf dry matter content. CV = coefficient of variation.

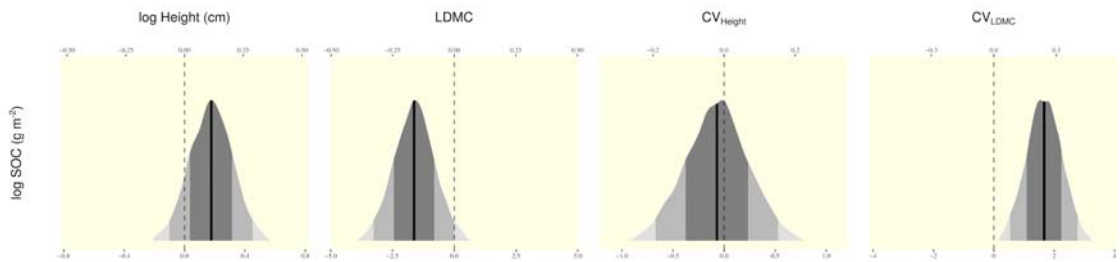

Fig. S4 Kernel density plots of the posterior distributions of trait effects on soil organic carbon stocks. The lower x-axis is on the original scale, while the upper axis depicts the effects as standardized regression coefficients. The black line depicts the mean, the dark gray area around it ±1 SD, the lighter dark gray the 95% CI, and the lightest gray the rest of the distribution. SOC = soil organic carbon stock. LDMC = leaf dry matter content. CV = coefficient of variation.

Methods S1 Correction of Light Quantum Sensor PAR values

In 2018 additional PAR measurements were done with three sensors to verify that macrotopography does not influence PAR measurements within the study area. PAR Light Quantum Sensors 3668I were placed near study locations on north- and south-facing slopes and in the valley.

The spectral range of the continuous Light Quantum Sensor (400-700 nm) was different compared to the handheld MQ-200 sensors (see section CO2 flux data), thus the PAR values in the Light Quantum Sensor were corrected based on seven comparative measurements in different light levels between the Light Quantum Sensor and MQ-200. Light Quantum Sensor PAR values were multiplied by 0.91 (R2 = 0.99). We arrived at this multiplier by regressing the MQ-200 values with Light Quantum Sensor values without the intercept.

Methods S2 Soil organic carbon stocks

C% and bulk density were analyzed from organic samples that were collected from 108 samples. Out of these sites, 13 had organic samples with C% and bulk density data from the same layer from the two sampling years (2016-2017), in which cases we took an average of the soil organic layer carbon stock across the two years. Due to the high costs of CNS analyzer runs, C% was not measured from all organic samples (n = 129). We measured soil organic matter content (SOM%) with loss on ignition method according to SFS 3008 from the remaining sites. We calculated soil organic matter stocks following Equation 2 and converted them into SOC based on the relationship between soil organic layer carbon and soil organic matter stocks. For this conversion, we used data from the study area that had both C% and SOM data from organic samples (n = 118). The carbon fraction in the soil organic matter was calculated as 0.54 (R2 = 0.97), similar to (Parker et al., 2015). This was then used to estimate the soil organic carbon stock in the organic layer. We arrived at this fraction by regressing the soil organic carbon stock in the organic soil layer using the soil organic matter stock in the organic soil layer without the intercept.

Methods S3 Light-response model

We fitted plot-specific light-response curves using a non-linear hierarchical bayesian model. We used the Michaelis-Menten equation to model the *n* instantaneous observations of NEE as a function of *k* plot-specific ER, maximum photosynthetic rate GPP_{max}, and the half-saturation constant K (Eqns S1 & S5). ER, GPP_{max} and K were allowed to have plot-specific averages (Eqns S2–S4 & S6–S8), and ER also had an exponential temperature (T) response (Eqn S2).

$$NEE_{ij} = -ER_{ij} + \left(\frac{GPP_{maxj}PAR_i}{K_j + PAR_i}\right) + e_{ij}, (i = i \ldots n, j = 1 \ldots k)$$ (Eqn S1)

$$log\left(ER_{ij}\right) = Intercept_{ER} + T_{ij}\beta_{Temperature} + u_{ERj}$$ (Eqn S2)

$$GPP_{maxj} = Intercept_{GPP} + u_{GPPj}$$ (Eqn S3)

$$log(K|j) = Intercept_K + u_{Kj}$$ (Eqn S4)

$$e \sim N(0, \sigma_{NEE})$$ (Eqn S5)

$$u_{ER} \sim N(0, \sigma_{ER})$$ (Eqn S6)

$$u_{GPP} \sim N(0, \sigma_{GPP})$$ (Eqn S7)

$$u_K \sim N(0, \sigma_K)$$ (Eqn S8)

The Michaelis-Menten parameters GPP_{max} and half-saturation constant K sometimes identify weakly, so that the data would be consistent with infinitely increasing photosynthesis. This is especially true when CO_2 fluxes are small, which is frequently the case in tundra ecosystems. To counter this, we set weakly informative priors on the plot-specific intercept terms based on visual inspection of the scale of variation in our data and typical parameter values reported in (Williams *et al.*, 2006) (Eqns S9–S11). A weakly informative prior was also set for the temperature effect on respiration $\beta_{Temperature}$ (Eqn S12). Priors for the variance parameters were left as the weakly informative *brms* defaults (Eqn S13).

$Intercept_{ER} \sim N(1,2)$ (Eqn S9)

$Intercept_{GPP} \sim N(10,10)$ (Eqn S10)

$Intercept_{K} \sim N(6.2,0.3)$ (Eqn S11)

$\beta_{Temperature} \sim N(0,1)$ (Eqn S12)

$\sigma_{ER}, \sigma_{GPP}, \sigma_{K,} \sigma_{NEE} \sim Student - t^{+}(3,10)$ (Eqn S13)

The model was fit with 4 Markov Chain Monte Carlo (MCMC) chains, which were run for 2000 iterations each. The first 1000 iterations were discarded as warmup, leaving a total of 4000 samples of each parameter.

References

Parker TC, Subke JA, Wookey PA. **2015**. Rapid carbon turnover beneath shrub and tree vegetation is associated with low soil carbon stocks at a subarctic treeline. *Global Change Biology* **21**: 2070–2081.

SFS 3008. 1990. Determination of total residues and total fixed residue in water, sludge and sediment. Finnish Standards Association (SFS).